

Published in final edited form as:

*Arch Neurol.* 2011 June ; 68(6): 753–760. doi:10.1001/archneurol.2011.107.

## Clinical correlates of white matter tract degeneration in PSP

Jennifer L. Whitwell, PhD<sup>1</sup>, Ankit V. Master, MS<sup>1</sup>, Ramesh Avula, PhD<sup>1</sup>, Kejal Kantarci, MD, MSc<sup>1</sup>, Scott D. Eggers, MD<sup>2</sup>, Heidi A. Edmonson, PhD<sup>1</sup>, Clifford R. Jack, MD<sup>1</sup>, and Keith A. Josephs, MD, MST, MSc<sup>2</sup>

<sup>1</sup>Department of Radiology, Mayo Clinic, 2001<sup>st</sup> Street SW, Rochester, MN, USA

<sup>2</sup>Department of Neurology (Behavioral Neurology), Mayo Clinic, 2001<sup>st</sup> Street SW, Rochester, MN, USA

### Abstract

**Objective**—Progressive supranuclear palsy (PSP) is associated with degeneration of white matter tracts that can be detected using diffusion tensor imaging (DTI). However, little is known about whether tract degeneration is associated with the clinical symptoms of PSP. The aim of this study was to use DTI to assess white matter tract degeneration in PSP and to investigate correlates, between tract integrity and clinical measures.

**Design**—Case-control study

**Setting**—Tertiary care medical centre

**Patients**—Twenty subjects with probable PSP and 20 age and gender-matched healthy controls. All PSP subjects underwent standardized clinical testing, including the Frontal Behavioral Inventory and Frontal Assessment Battery to assess behavioral change; the PSP Rating Scale to measure disease severity, the Movement Disorder Society-sponsored revision of the Unified Parkinson's Disease Rating Scale (parts I, II and III) to measure motor function, and the PSP Saccadic Impairment Scale to measure eye movement abnormalities.

**Main outcome measures**—Fractional anisotropy and mean diffusivity measured using both region-of-interest analysis and Track Based Spatial Statistics.

**Results**—Abnormal diffusivity was observed predominantly in superior cerebellar peduncles, body of the corpus callosum, inferior longitudinal fasciculus and superior longitudinal fasciculus in PSP compared to controls. Fractional anisotropy values in the superior cerebellar peduncles correlated with disease severity; inferior longitudinal fasciculus correlated with motor function, and superior longitudinal fasciculus correlated with severity of saccadic impairments.

**Conclusions**—These results demonstrate that PSP is associated with degeneration of brainstem, association and commissural fibers and that this degeneration likely plays an important role in clinical dysfunction.

## INTRODUCTION

Progressive supranuclear palsy (PSP) is a neurodegenerative disorder characterized by a symmetrical akinetic-rigid syndrome with vertical supranuclear gaze palsy and early falls<sup>1,2</sup>. It is characterized by deposition of tau<sup>3</sup>, with pathological findings and degeneration affecting the white matter, particularly brainstem tracts<sup>3,4</sup>, with less involvement of the cortex. Imaging studies have similarly found more severe involvement of

white matter than cortical grey matter in PSP<sup>5-7</sup>. White matter tract degeneration is therefore likely to be contributing to many clinical symptoms observed in subjects with PSP.

The integrity of specific white matter tracts can be assessed using diffusion tensor imaging (DTI), which measures water diffusion in the brain and can measure directional information and visualize specific white matter tracts. A few DTI studies have been performed in PSP and have demonstrated abnormalities in the superior cerebellar peduncles<sup>8-10</sup>, cingulate gyrus<sup>9</sup>, and corpus callosum<sup>10-12</sup>, although these previous studies failed to identify correlations between these tracts and clinical features in PSP<sup>8, 12</sup>, likely due to small numbers of subjects. In addition, these previous studies did not investigate correlations between clinical measures and degeneration of association fibers in PSP.

The aim of this study was to investigate white matter tract abnormalities in a large, well characterized cohort of PSP subjects and to assess correlations between white matter tract integrity and performance on a number of different standardized and validated clinical scales. We used carefully placed regions-of-interest (ROIs) to measure directional water diffusion (fractional anisotropy (FA)) and mean diffusivity (MD) on specific tracts, including superior cerebellar peduncle, corticospinal and corticobulbar tracts. In addition, since PSP has been associated with neocortical volume loss we also assessed corpus callosum and multiple association fibers. In order to provide independent validation of the ROI-based findings we assessed voxel-level abnormalities in white matter tracts using the automated and unbiased technique of Tract-Based Spatial Statistics (TBSS).

## METHODS

### Subjects

Twenty subjects that met clinical research criteria for probable PSP<sup>1</sup> were included in this study. All subjects with PSP that were evaluated in the Department of Neurology, Mayo Clinic, between August 1<sup>st</sup> 2009 and April 30<sup>th</sup> 2010 were consecutively recruited (n=26) into a prospective longitudinal PSP study by a neurodegenerative specialist and PSP expert (KAJ). All subjects underwent 3T DTI scanning with 42 directions and detailed clinical evaluations. For this study, only patients meeting criteria for probable PSP<sup>1</sup> were analyzed since probable PSP diagnosis has high positive predictive value (100%) for the diagnosis of PSP<sup>13</sup>. Subjects were excluded from the study if they only met possible criteria for PSP<sup>1</sup>, did not consent to perform a 3.0 Tesla MRI, if MRI was contraindicated or if the MRI revealed a lesion that would affect final analysis, such a large stroke, tumor or hemorrhage.

All subjects underwent clinical and neurological examination and completed standardized and validated testing with the following batteries: Mini-Mental State Examination (MMSE)<sup>14</sup>, Frontal Behavioral Inventory (FBI)<sup>15</sup>, Frontal Assessment Battery (FAB)<sup>16</sup>; PSP Rating Scale (PSPRS)<sup>17</sup>, and Movement Disorder Society-sponsored revision of the Unified Parkinson's Disease Rating Scale (parts I, II and III) (MDS-UPDRS)<sup>18</sup>. Eye saccades were also graded using a 5-point scale completed using clinical impression (The PSP Saccadic Impairment scale (PSIS), See Box 1).

#### Box 1

##### PSP Saccadic Impairment scale (PSIS)

0 = normal vertical and horizontal saccades

1 = Mild slowing of upward or downward saccades

2 = Moderate slowing of upward and downwards saccades

3 = Severe slowing or absence of both upwards and downwards saccades with or without mild slowing of horizontal saccades

4 = Severe slowing or absence of vertical saccades and moderate to severe slowing of horizontal saccades

5 = Complete vertical and horizontal saccadic palsy

Twenty healthy control subjects that were age and gender-matched to the PSP cohort were also prospectively recruited. All controls performed within normal limits on standardized neurological and neuropsychological testing and had the same DTI acquisition sequence as the PSP cohort.

### Image acquisition

A standardized protocol was performed on a 3T GE scanner. The DTI acquisition consisted of a single-shot echo-planar (EPI) pulse sequence in the axial plane, with TR= 10,200ms; in-plane matrix 128/128; FOV 35 cm; phase FOV 0.66; 42 diffusion encoding steps and four non-diffusion weighted T2 images; slice thickness 2.7mm (2.7m isotropic resolution). Parallel imaging with a SENSE factor of two was used. Each of the 42 diffusion-weighted images was registered to the non-diffusion weighted b0 volumes using affine transformations to minimize distortions due to eddy currents.

### ROI analysis

Maps of fractional anisotropy (FA), color-coded FA, and mean diffusivity (MD) were computed from these 42 diffusion-weighted images using DTIstudio<sup>19</sup>. Regions-of-interest were placed on specific tracts on the color-coded FA maps using Analyze software by one rater (JLW) blinded to clinical diagnosis. Regions were placed using anatomical landmarks on axial images with coronal and sagittal images viewed simultaneously to guide placement. In order to assess brainstem white matter tracts, ROIs were placed on corticospinal tracts and middle cerebellar peduncles at the level of the pons and in the superior cerebellar peduncles at the level of the decussation (Figure 1). Projection fibers were assessed with ROIs in the anterior limb, genu and posterior limb of the internal capsule (Figure 1). Two ROIs were placed in the posterior limb: one in the lateral rostral third to sample the corticofugal fibers/superior thalamic radiation, and the other positioned laterally in the caudal third in order to sample the corticospinal tracts. Association fibers were assessed with ROIs placed in the inferior longitudinal fasciculus, uncinate fasciculus, superior longitudinal fasciculus and anterior and posterior cingulum bundle. The superior longitudinal fasciculus was sampled at three positions: anterior descending tracts branching into the inferior frontal lobes; posterior descending tracts branching into posterior temporal lobes, and superior horizontal fibers usually positioned adjacent to the most superior slice of the lateral ventricles. ROIs were also placed on the corpus callosum, including genu, splenium and uppermost portion of the body. The location of many of these ROIs have been previously illustrated<sup>20</sup>. The selection of these ROIs was performed independently from, and prior to the completion of, the TBSS analysis, and was based on previous literature. We have previously demonstrated excellent inter-rater reproducibility for these ROI measurements<sup>20</sup>.

All ROIs were measured separately for left and right hemispheres, except for corpus callosum. Once the ROIs had been placed using color-coded FA maps they were overlaid on FA and MD maps to calculate mean FA and MD for each ROI. Due to the potential problem of partial volume affects the maximum FA from each ROI was also assessed.

## TBSS

Images were brain-extracted using the BET<sup>21</sup> utility from the FSL package<sup>22</sup>. FA and MD maps were generated using FSL Diffusion Toolbox<sup>23</sup>. Voxel-wise statistical analysis of FA and MD data was performed using TBSS<sup>24</sup> (<http://www.fmrib.ox.ac.uk/fsl>). The FA images for each subject were first aligned into a common space using the non-linear registration tool IRTK<sup>25</sup>. The subject that was the most representative subject from the entire group was selected automatically as the target and FA images of all other subjects were non-linearly aligned to it. Following this step, all images were affinely transformed into MNI space. A mean FA image was created from all subjects in this study, and this mean image was thinned to create a mean FA skeleton which represents the centers of all tracts common to the group. The FA skeleton was thresholded at  $>0.25$  to include the major white matter pathways but exclude peripheral tracts where there was significant inter-subject variability and/or partial volume effects with grey matter and CSF. Each subject's aligned FA data was then projected onto this skeleton and the resulting data were fed into voxel-wise cross-subject statistics. The transformations applied to the FA images were also applied to the MD images and tract-based statistics were calculated for MD. Two-sample two-sided t-tests were performed using both FA and MD images to compare PSP and controls. Results were assessed after correction for multiple comparisons using family-wise error correction at  $p < 0.05$ .

## Statistics

Statistical analyses were performed utilizing the JMP computer software (JMP Software, version 6.0.0; SAS Institute Inc, Cary, NC) with  $\alpha$  set at 0.05. A chi-square test was used to compare categorical data across groups of interest. Two sample t-tests assuming unequal variances were used to compare continuous data between groups. For any ROIs that showed significant findings or trends in the PSP group when compared to controls, we also performed a pair-wise correlation analysis between both FA and MD values and scores on the MMSE, PSPRS, FBI, FAB, PSIS and MDS-UPDRS. Linear regression analysis was used to adjust for disease severity. Receiver operating characteristic (ROC) curve analysis was used to assess diagnostic specificity and sensitivity.

## RESULTS

### Subject demographics

Subject demographics and clinical test scores are shown in Table 1. There was no significant difference between PSP and controls in gender ratio, age at MRI or education.

### Group comparisons

The ROI-based results of FA and MD for the PSP subjects and controls are shown in Table 2 and Figure 2. No differences were observed between the left and right volumes and therefore an average was used for further analysis. The PSP subjects showed decreased FA and increased MD in the superior cerebellar peduncles, superior portion of the superior longitudinal fasciculus and body of the corpus callosum, with decreased FA also observed in the anterior superior longitudinal fasciculus and inferior longitudinal fasciculus, and increased MD in the genu of the internal capsule. The same trends for differences across groups were identified when the maximum FA values were assessed. The superior cerebellar peduncle showed the most dramatic differences between PSP and controls, and provided excellent discrimination between groups (area under ROC curve of 0.96 for FA and 0.92 for MD). For a specificity of 95%, FA had a sensitivity of 85% (cut point 0.75) and MD had a sensitivity of 80% (cut point  $631 \times 10^{-6} \text{ mm}^2/\text{sec}$ ) in differentiating PSP from controls. Supplemental Figure 1 shows the superior cerebellar peduncle ROI overlaid on FA images for a selection of PSP and control subjects.

Similar findings were observed with the TBSS analysis (Figure 3), with the PSP subjects once again showing reduced FA in superior cerebellar peduncles, body of the corpus callosum, anterior and superior aspects of the superior longitudinal fasciculus and inferior longitudinal fasciculus. Some additional regions of reduced FA were also observed in pontine crossing fibers, cerebral peduncles, fornix, optic tract and thalamus. No regions of increased MD were observed in the PSP subjects compared to controls after correction for multiple comparisons. No regions were identified that showed decreased FA or increased MD in the controls compared to PSP either with or without correction for multiple comparisons.

### Clinical correlations

Significant correlations were observed between the FA values in the superior cerebellar peduncles and performance on the FBI ( $r=-0.48$ ,  $p=0.03$ ), PSPRS ( $r=-0.59$ ,  $p=0.006$ ), MMSE ( $r=0.48$ ,  $p=0.03$ ), MDS-UPDRS I ( $r=-0.49$ ,  $p=0.03$ ), MDS-UPDRS II ( $r=-0.54$ ,  $p=0.01$ ), and MDS-UPDRS III ( $r=-0.47$ ,  $p=0.04$ ) (Figure 4). However, the relationships between the superior cerebellar peduncles and the FBI, MMSE, MDS-UPDRS I, MDS-UPDRS II and MDS-UPDRS III were not significant when the analyses were adjusted for PSPRS, i.e. disease severity. Significant correlations were observed between both FA and MD values in the inferior longitudinal fasciculus and performance on the MDS-UPDRS II (FA:  $r=-0.51$ ,  $p=0.02$ , MD:  $r=0.55$ ,  $p=0.01$ ) and MDS-UPDRS III (FA:  $r=-0.47$ ,  $p=0.04$ , MD:  $r=0.45$ ,  $p=0.05$ ) (Figure 4). A significant correlation was also observed between the anterior portion of the superior longitudinal fasciculus and the PSIS ( $r=-0.45$ ,  $p=0.047$ ). This correlation was improved when the outlier subject in Figure 4 was removed ( $r=-0.60$ ,  $p=0.007$ ), and remained significant after adjusting for disease severity ( $p=0.03$ ). Time from onset to scan did not correlate to any of the DTI ROI measurements.

### COMMENT

This study demonstrates white matter tract degeneration in the superior cerebellar peduncles, corpus callosum, and association fibers in PSP and shows that this degeneration is associated with clinical dysfunction in PSP.

The superior cerebellar peduncles were the tracts that showed the most significant decreases in FA and increases in MD in PSP compared to controls, and provided excellent discrimination between groups. This finding confirms previous DTI studies<sup>8–10, 26</sup>, and concurs with the fact that demyelination and microgliosis have both been observed in these structures at pathology<sup>2, 27, 28</sup>. Volume loss of the superior cerebellar peduncles has also been observed in PSP<sup>4, 29, 30</sup>. This finding contrasts with the relative preservation of the middle cerebellar peduncle. In this study we found significant correlations between FA values in the superior cerebellar peduncles and performance on tests of disease severity, including the PSPRS, FBI, MMSE and MDS-UPDRS. While each of these tests measures different aspects of motor, cognitive and behavioral ability, they were all highly correlated to PSPRS suggesting that performance on each test is associated with disease severity. Our results therefore suggest that FA measures in the superior cerebellar peduncle could be an excellent marker of disease severity in PSP. These results also demonstrate disruption of the dentatorubrothalamic tract which runs through the superior cerebellar peduncles to the contralateral ventrolateral nucleus of the thalamus<sup>31</sup>. In fact, the TBSS analysis demonstrated reduced FA in the thalamus which likely reflects degeneration of this system. While the thalamus is predominantly a grey matter structure and so was not sampled in the ROI-based analysis, it does contain a system of myelinated fibers (internal medullary lamina) that separate thalamic subdivisions<sup>32</sup> and were likely detected by TBSS. Previous studies have only been able to demonstrate increased MD in the grey matter of the thalamus in PSP<sup>9, 33, 34</sup>.

Significantly reduced FA and increased MD were also both observed in the body of the corpus callosum in PSP, yet no changes were observed in the splenium or genu. These findings may reflect degeneration of the commissural fibers connecting adjacent regions of grey matter loss in the posterior frontal and premotor cortex that are commonly observed in PSP<sup>6</sup>. Previous studies have similarly identified changes in diffusivity and volume loss in anterior-middle portions of the corpus callosum<sup>11, 12, 26, 35, 36</sup>. Measurements of FA and MD in the body of the corpus callosum did not correlate with any clinical measures however suggesting that it is not directly associated with the clinical symptoms of PSP.

Diffusivity changes were also observed in association fibers, namely the inferior longitudinal fasciculus and superior longitudinal fasciculus. Correlations were identified between both FA and MD values in inferior longitudinal fasciculus and scores on the MDS-UPDRS parts II and III which assess motor function. Interestingly, a couple of recent DTI studies investigating healthy aging have similarly found associations between abnormalities in the inferior longitudinal fasciculus and motor function<sup>37</sup> and visuomotor dexterity<sup>38</sup>. The inferior longitudinal fasciculus connects visual cortices to the inferior, middle and superior temporal lobes, and has been suggested to subserve a “direct short-latency pathway” of visual processing<sup>39</sup>. Visual-motor coordination is indeed likely to play a role in performance on a number of the items assessed using the MDS-UPDRS, such as toe and finger tapping and hand movements. Performance on the MDS-UPDRS parts II and III did however also correlate with diffusivity in the superior cerebellar peduncles suggesting that motor function may involve a complex network of systems in PSP.

Reductions in FA were observed in both the anterior descending tracts and the horizontal superior tracts of the superior longitudinal fasciculus. These tracts project to the posterior frontal lobes; regions that are atrophic in PSP<sup>6</sup>. Anterior superior longitudinal fasciculus FA correlated with performance on the PSP Saccadic Impairment Scale which attempts to grade severity of eye movement abnormalities that occur in PSP (Box 1). This is a novel finding, yet plausible since although several structures in the brainstem determine the direction, amplitude, and velocity of saccades<sup>40, 41</sup>, fMRI and PET studies demonstrate that voluntary saccades are under cortical control<sup>42, 43</sup> and the frontal and supplemental eye fields are known to play a role in saccadic eye movements<sup>44</sup>. Our results suggest a possible cortical element to saccadic abnormalities in PSP, perhaps involving the frontal eye fields and premotor cortices, mediated by the superior longitudinal fasciculus.

It is clear from the TBSS analysis that reductions in FA were more severe than increases in MD in our PSP cohort, suggesting that directional diffusivity, and hence degeneration of the white matter tracts, is predominantly affected in PSP. There are a number of pathological mechanisms which could be contributing to breakdown of diffusion along white matter tracts: 1) tau deposition observed within axons and the outer mesaxon of myelinated fibers<sup>3, 45, 46</sup>, 2) phagocytosis of myelin by macrophages (activate microglia) that are found in white matter tracts in PSP<sup>27, 47</sup>, and 3) wallerian degeneration. The degree of demyelination in the superior cerebellar peduncle has been shown to correlate to tau burden, not microglial burden, in PSP<sup>27</sup>, suggesting that tau pathology may be responsible for the degeneration of white matter tracts although further pathological studies will be needed in order to understand these biological mechanisms.

Strengths of this manuscript include the fact that all patients were prospectively assessed with a standardized battery of clinical assessments and the number of subjects was large, especially for a rare disorder like PSP. In addition, we utilized two independent DTI analysis techniques. One could argue that results from small ROIs placed on specific tracts may not be representative of the entire tract, although the similarity across the ROI-based and TBSS analyses supported the validity of the data. Furthermore, the TBSS analysis showed



significant findings after correction for multiple comparisons, increasing confidence in the results. A limitation of using DTI to assess white matter tract dysfunction in PSP, however, is that the resolution of the scans limits the ability to identify and measure very small tracts that may also be playing important roles in the disease, such as the subthalamic fasciculus connecting subthalamic nuclei to basal ganglia. Our analysis of maximum FA demonstrated that the ROI results were unlikely to be confounded by partial volume averaging, although this could still be a problem in the TBSS analysis for thin tracts such as the fornix.

## CONCLUSIONS

This study has provided a detailed characterization of the patterns of white matter tract degeneration in subjects with PSP and demonstrated correlations between these patterns and clinical symptoms. Abnormal diffusivity was observed within brainstem tracts, such as the superior cerebellar peduncles, as well as in the body of the corpus callosum and some association fibers. Degeneration of the superior cerebellar peduncles seems to be an excellent marker of disease severity in PSP. In addition, degeneration of the inferior longitudinal fasciculus appears to be associated with motor function, while the superior longitudinal fasciculus appears to be associated with ocular motor abnormalities.

## Supplementary Material

Refer to Web version on PubMed Central for supplementary material.

## Acknowledgments

The study was funded by the Dana Foundation, a Mayo Clinic Departmental Small Grant, NIA R01-AG11378 and K23 AG030935. The funding source had no involvement in the study design, collection, interpretation and analysis of data, in writing the report, or in the decision to submit the manuscript. We would like to thank Brian Gregg and Matthew L. Senjem, MS, for assistance in DTI processing, and Stephen D. Weigand, MS, for creating the box-plots.

## References

1. Litvan I, Agid Y, Calne D, et al. Clinical research criteria for the diagnosis of progressive supranuclear palsy (Steele-Richardson-Olszewski syndrome): report of the NINDS-SPSP international workshop. *Neurology*. 1996; 47:1–9. [PubMed: 8710059]
2. Steele JC, Richardson JC, Olszewski J. Progressive Supranuclear Palsy. a Heterogeneous Degeneration Involving the Brain Stem, Basal Ganglia and Cerebellum with Vertical Gaze and Pseudobulbar Palsy, Nuchal Dystonia and Dementia. *Arch Neurol*. 1964; 10:333–359. [PubMed: 14107684]
3. Hauw JJ, Daniel SE, Dickson D, et al. Preliminary NINDS neuropathologic criteria for Steele-Richardson-Olszewski syndrome (progressive supranuclear palsy). *Neurology*. 1994; 44:2015–2019. [PubMed: 7969952]
4. Tsuboi Y, Slowinski J, Josephs KA, et al. Atrophy of superior cerebellar peduncle in progressive supranuclear palsy. *Neurology*. 2003; 60:1766–1769. [PubMed: 12796528]
5. Boxer AL, Geschwind MD, Belfor N, et al. Patterns of brain atrophy that differentiate corticobasal degeneration syndrome from progressive supranuclear palsy. *Archives of neurology*. 2006; 63:81–86. [PubMed: 16401739]
6. Josephs KA, Whitwell JL, Dickson DW, et al. Voxel-based morphometry in autopsy proven PSP and CBD. *Neurobiol Aging*. 2008; 29:280–289. [PubMed: 17097770]
7. Price S, Paviour D, Scahill R, et al. Voxel-based morphometry detects patterns of atrophy that help differentiate progressive supranuclear palsy and Parkinson's disease. *Neuroimage*. 2004; 23:663–669. [PubMed: 15488416]
8. Blain CR, Barker GJ, Jarosz JM, et al. Measuring brain stem and cerebellar damage in parkinsonian syndromes using diffusion tensor MRI. *Neurology*. 2006; 67:2199–2205. [PubMed: 17190944]

9. Erbetta A, Mandelli ML, Savoiardo M, et al. Diffusion tensor imaging shows different topographic involvement of the thalamus in progressive supranuclear palsy and corticobasal degeneration. *Ajnr*. 2009; 30:1482–1487. [PubMed: 19589886]
10. Nilsson C, Markenroth Bloch K, Brockstedt S, et al. Tracking the neurodegeneration of parkinsonian disorders--a pilot study. *Neuroradiology*. 2007; 49:111–119. [PubMed: 17200869]
11. Ito S, Makino T, Shirai W, Hattori T. Diffusion tensor analysis of corpus callosum in progressive supranuclear palsy. *Neuroradiology*. 2008; 50:981–985. [PubMed: 18779957]
12. Padovani A, Borroni B, Brambati SM, et al. Diffusion tensor imaging and voxel based morphometry study in early progressive supranuclear palsy. *Journal of neurology, neurosurgery, and psychiatry*. 2006; 77:457–463.
13. Lopez OL, Litvan I, Catt KE, et al. Accuracy of four clinical diagnostic criteria for the diagnosis of neurodegenerative dementias. *Neurology*. 1999; 53:1292–1299. [PubMed: 10522887]
14. Folstein MF, Robins LN, Helzer JE. The Mini-Mental State Examination. *Archives of general psychiatry*. 1983; 40:812. [PubMed: 6860082]
15. Kertesz A, Davidson W, Fox H. Frontal behavioral inventory: diagnostic criteria for frontal lobe dementia. *The Canadian journal of neurological sciences*. 1997; 24:29–36. [PubMed: 9043744]
16. Dubois B, Slachevsky A, Litvan I, Pillon B. The FAB: a Frontal Assessment Battery at bedside. *Neurology*. 2000; 55:1621–1626. [PubMed: 11113214]
17. Golbe LI, Ohman-Strickland PA. A clinical rating scale for progressive supranuclear palsy. *Brain*. 2007; 130:1552–1565. [PubMed: 17405767]
18. Goetz CG, Fahn S, Martinez-Martin P, et al. Movement Disorder Society-sponsored revision of the Unified Parkinson's Disease Rating Scale (MDS-UPDRS): Process, format, and clinimetric testing plan. *Mov Disord*. 2007; 22:41–47. [PubMed: 17115387]
19. Jiang H, van Zijl PC, Kim J, et al. DtiStudio: resource program for diffusion tensor computation and fiber bundle tracking. *Comput Methods Programs Biomed*. 2006; 81:106–116. [PubMed: 16413083]
20. Whitwell JL, Avula R, Senjem ML, et al. Gray and white matter water diffusion in the syndromic variants of frontotemporal dementia. *Neurology*. 2010; 74:1279–1287. [PubMed: 20404309]
21. Smith SM. Fast robust automated brain extraction. *Human brain mapping*. 2002; 17:143–155. [PubMed: 12391568]
22. Smith SM, Jenkinson M, Woolrich MW, et al. Advances in functional and structural MR image analysis and implementation as FSL. *NeuroImage*. 2004; 23 (Suppl 1):S208–219. [PubMed: 15501092]
23. Behrens TE, Woolrich MW, Jenkinson M, et al. Characterization and propagation of uncertainty in diffusion-weighted MR imaging. *Magn Reson Med*. 2003; 50:1077–1088. [PubMed: 14587019]
24. Smith SM, Jenkinson M, Johansen-Berg H, et al. Tract-based spatial statistics: voxelwise analysis of multi-subject diffusion data. *NeuroImage*. 2006; 31:1487–1505. [PubMed: 16624579]
25. Rueckert D, Sonoda LI, Hayes C, et al. Nonrigid registration using free-form deformations: application to breast MR images. *IEEE transactions on medical imaging*. 1999; 18:712–721. [PubMed: 10534053]
26. Knake S, Belke M, Menzler K, et al. In vivo demonstration of microstructural brain pathology in progressive supranuclear palsy: A DTI study using TBSS. *Mov Disord*. 2010
27. Ishizawa K, Lin WL, Tiseo P, et al. A qualitative and quantitative study of grumose degeneration in progressive supranuclear palsy. *Journal of neuropathology and experimental neurology*. 2000; 59:513–524. [PubMed: 10850864]
28. Behrman S, Carroll JD, Janota I, Matthews WB. Progressive supranuclear palsy. Clinico-pathological study of four cases. *Brain*. 1969; 92:663–678. [PubMed: 5806130]
29. Paviour DC, Price SL, Stevens JM, et al. Quantitative MRI measurement of superior cerebellar peduncle in progressive supranuclear palsy. *Neurology*. 2005; 64:675–679. [PubMed: 15728291]
30. Slowinski J, Imamura A, Uitti RJ, et al. MR imaging of brainstem atrophy in progressive supranuclear palsy. *Journal of neurology*. 2008; 255:37–44. [PubMed: 18080856]
31. Voogd J, Feirabend, HKP.; Schoen, JHR. Cerebellum and precerebellar nuclei. In: Paxinos, G., editor. *The human nervous system*. San Diego: Academic Press Inc; 1990. p. 321–386.



32. Parent, A. *Carpenter's Human Neuroanatomy*. 9. Media, PA: Williams and Wilkins; 1996.
33. Nicoletti G, Lodi R, Condino F, et al. Apparent diffusion coefficient measurements of the middle cerebellar peduncle differentiate the Parkinson variant of MSA from Parkinson's disease and progressive supranuclear palsy. *Brain*. 2006; 129:2679–2687. [PubMed: 16815875]
34. Paviour DC, Thornton JS, Lees AJ, Jager HR. Diffusion-weighted magnetic resonance imaging differentiates Parkinsonian variant of multiple-system atrophy from progressive supranuclear palsy. *Mov Disord*. 2007; 22:68–74. [PubMed: 17089396]
35. Yamauchi H, Fukuyama H, Nagahama Y, et al. Atrophy of the corpus callosum, cognitive impairment, and cortical hypometabolism in progressive supranuclear palsy. *Annals of neurology*. 1997; 41:606–614. [PubMed: 9153522]
36. Yamauchi H, Fukuyama H, Nagahama Y, et al. Comparison of the pattern of atrophy of the corpus callosum in frontotemporal dementia, progressive supranuclear palsy, and Alzheimer's disease. *Journal of neurology, neurosurgery, and psychiatry*. 2000; 69:623–629.
37. Zahr NM, Rohlfing T, Pfefferbaum A, Sullivan EV. Problem solving, working memory, and motor correlates of association and commissural fiber bundles in normal aging: a quantitative fiber tracking study. *NeuroImage*. 2009; 44:1050–1062. [PubMed: 18977450]
38. Voineskos AN, Rajji TK, Lobaugh NJ, et al. Age-related decline in white matter tract integrity and cognitive performance: A DTI tractography and structural equation modeling study. *Neurobiol Aging*. 2010 [Epub].
39. Catani M, Jones DK, Donato R, Ffytche DH. Occipito-temporal connections in the human brain. *Brain*. 2003; 126:2093–2107. [PubMed: 12821517]
40. Revesz T, Sangha H, Daniel SE. The nucleus raphe interpositus in the Steele-Richardson-Olszewski syndrome (progressive supranuclear palsy). *Brain*. 1996; 119 ( Pt 4):1137–1143. [PubMed: 8813278]
41. Bhidayasiri R, Plant GT, Leigh RJ. A hypothetical scheme for the brainstem control of vertical gaze. *Neurology*. 2000; 54:1985–1993. [PubMed: 10822441]
42. Bodis-Wollner I, Bucher SF, Seelos KC. Cortical activation patterns during voluntary blinks and voluntary saccades. *Neurology*. 1999; 53:1800–1805. [PubMed: 10563631]
43. Sweeney JA, Mintun MA, Kwee S, et al. Positron emission tomography study of voluntary saccadic eye movements and spatial working memory. *Journal of neurophysiology*. 1996; 75:454–468. [PubMed: 8822570]
44. Pflugshaupt T, Nyffeler T, von Wartburg R, et al. Loss of exploratory vertical saccades after unilateral frontal eye field damage. *J Neurol Neurosurg Psychiatry*. 2008; 79:474–477. [PubMed: 17951279]
45. Josephs KA, Mandrekar JN, Dickson DW. The relationship between histopathological features of progressive supranuclear palsy and disease duration. *Parkinsonism & related disorders*. 2006; 12:109–112. [PubMed: 16337422]
46. Dickson DW. Neuropathologic differentiation of progressive supranuclear palsy and corticobasal degeneration. *Journal of neurology*. 1999; 246(Suppl 2):II6–15. [PubMed: 10525997]
47. Josephs KA, Katsuse O, Beccano-Kelly DA, et al. Atypical progressive supranuclear palsy with corticospinal tract degeneration. *Journal of neuropathology and experimental neurology*. 2006; 65:396–405. [PubMed: 16691120]

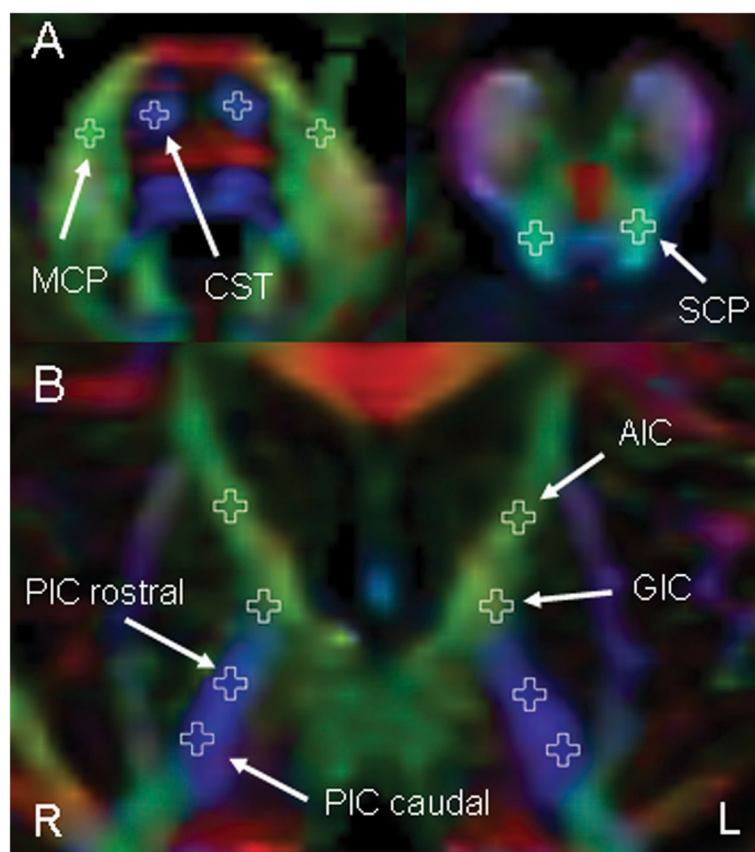


**Figure 1.**

FA color map from a control subject illustrating the placement of the brainstem (A) and internal capsule (B) white matter tract regions-of-interest. Regions-of-interest have been placed in both the left and right hemisphere. CST = corticospinal tracts, MCP = middle cerebellar peduncle; SCP = superior cerebellar peduncle; AIC = anterior limb of the internal capsule, GIC = genu of the internal capsule, PIC = posterior limb of the internal capsule.

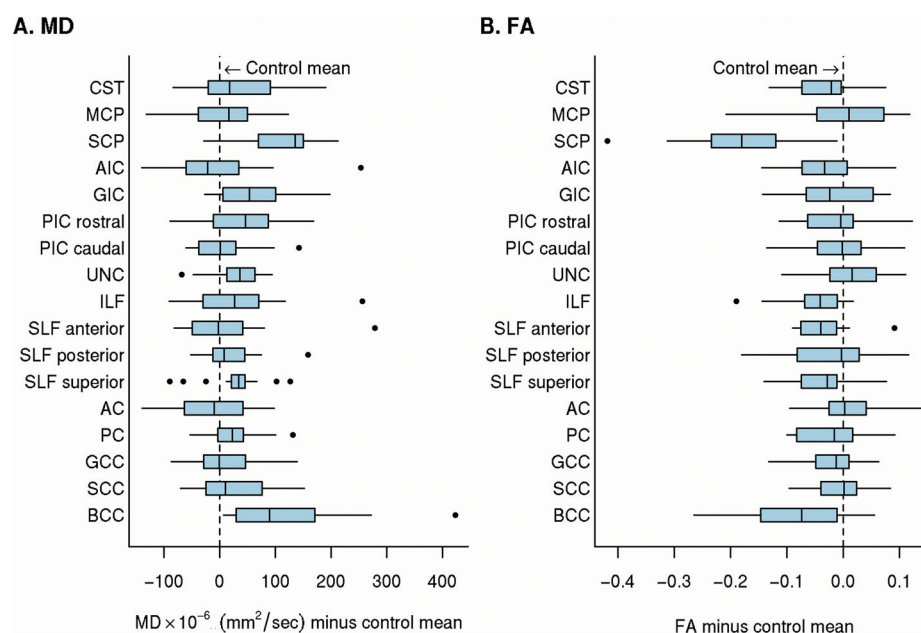


**Figure 2.**

Box-plots showing the distribution of FA and MD values for the PSP subjects. To aid comparison, FA and MD values were centered at the ROI-specific control group mean (defined as zero on the horizontal axis) and thus can be interpreted as differences between PSP and controls for each white matter tract ROI. The boxes indicate the 25<sup>th</sup>, 50<sup>th</sup> (median), and 75<sup>th</sup> percentiles of the distributions while the horizontal lines extending from the boxes stop at the most extreme data points. CST = corticospinal tracts at the level of the pons; MCP = middle cerebellar peduncle; SCP = superior cerebellar peduncle; GIC = genu of the internal capsule; PIC = posterior limb of the internal capsule; UNC = uncinate fasciculus; ILF = inferior longitudinal fasciculus; SLF = superior longitudinal fasciculus; AC = anterior cingulate; PC = posterior cingulate; GCC = genu of corpus callosum; SCC = splenium of corpus callosum; BCC = body of corpus callosum.

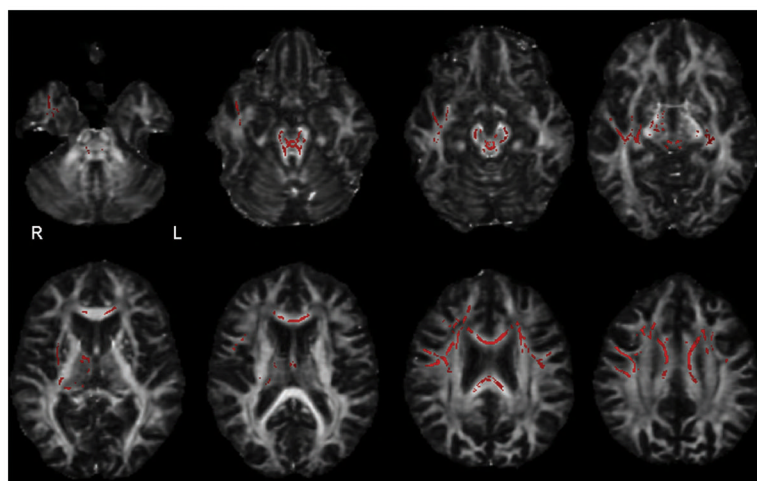


**Figure 3.** Regions of decreased FA observed in the PSP subjects compared to controls using TBSS. Results are shown after correction for multiple comparisons using the FWE at  $p < 0.05$ .

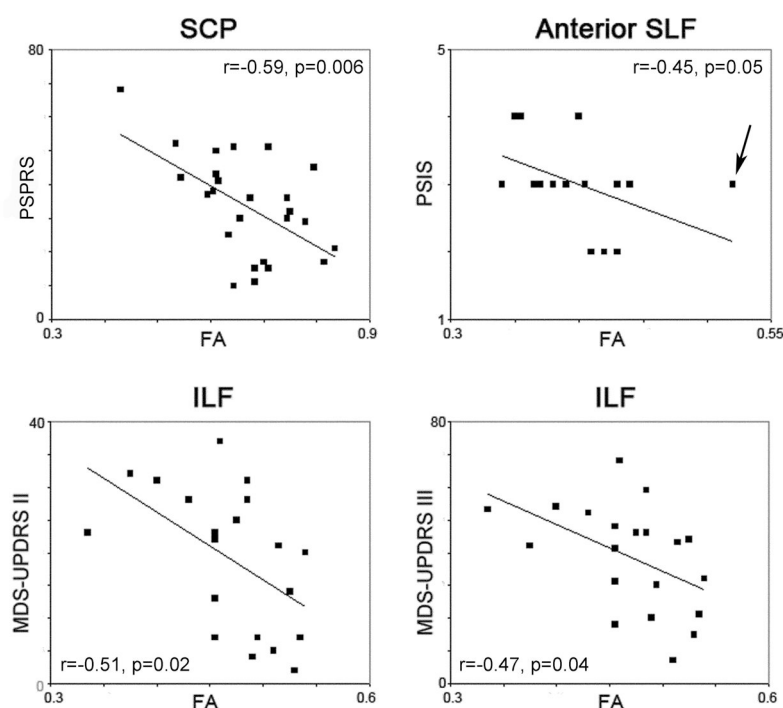


**Figure 4.** Scatter-plots with least-squares lines showing significant correlations between FA values and clinical measures in the PSP subjects. An outlier subject in the anterior SLF versus PSIS correlation is highlighted by an arrow. Once this outlier was removed the correlation improved ( $r = -0.60$ ,  $p = 0.007$ ). SCP = superior cerebellar peduncle; ILF = inferior longitudinal fasciculus; SLF = superior longitudinal fasciculus; PSPRS = PSP Rating Scale; PSIS = PSP Saccadic Impairment Scale; MDS-UPDRS = Unified Parkinson's Disease Rating Scale

**Table 1**

Subject demographics and clinical characteristics of all PSP subjects

	Controls (n=20)	PSP (n=20)
Gender (% female)	11 (55%)	10 (50%)
Education (yrs)	14.9 $\pm$ 2.9	14.5 $\pm$ 2.5
Age at exam (yrs)	69.4 $\pm$ 7.3	68.3 $\pm$ 7.2
Age at onset (yrs)	NA	64.7 $\pm$ 6.9
Time onset to exam (yrs)	NA	3.6 $\pm$ 1.8
FBI (/72)	NA	11.2 $\pm$ 11.4
FAB (/18)	NA	13.7 $\pm$ 2.1
PSPRS (/100)	NA	35.5 $\pm$ 15.7
PSIS (/5)	NA	3.1 $\pm$ 0.7
MMSE (/30)	NA	27.3 $\pm$ 3.7
MDS-UPDRS I (/52)	NA	10.0 $\pm$ 4.6
MDS-UPDRS II (/52)	NA	19.0 $\pm$ 10.8
MDS-UPDRS III (/132)	NA	38.5 $\pm$ 16.2

FBI = Frontal Behavioral Inventory; FAB = Frontal Assessment Battery; PSPRS = PSP Rating Scale; PSIS = PSP Saccadic Impairment Scale; MMSE = Mini-Mental State Examination; MDS-UPDRS = Unified Parkinson's Disease Rating Scale



**Table 2**

ROI-based FA and MD results for the PSP subjects and controls

	FA		P value	MD		P value
	Control (n=20)	PSP (n=20)		Control (n=20)	PSP (n=20)	
CST	0.62 ± 0.08	0.59 ± 0.05	0.12	681 ± 65	717 ± 81	0.13
MCP	0.79 ± 0.10	0.79 ± 0.09	0.86	623 ± 47	630 ± 64	0.71
SCP	0.85 ± 0.05	0.67 ± 0.10	<b>&lt;0.001</b>	577 ± 40	690 ± 62	<b>&lt;0.001</b>
AIC	0.57 ± 0.08	0.54 ± 0.07	0.22	755 ± 82	750 ± 86	0.86
GIC	0.62 ± 0.07	0.60 ± 0.07	0.45	723 ± 58	785 ± 70	<b>0.005</b>
PIC rostral	0.66 ± 0.05	0.64 ± 0.06	0.45	695 ± 64	734 ± 72	0.08
PIC caudal	0.67 ± 0.04	0.66 ± 0.06	0.69	725 ± 67	732 ± 53	0.71
UNC	0.48 ± 0.08	0.49 ± 0.06	0.51	710 ± 85	743 ± 44	0.13
ILF	0.52 ± 0.04	0.47 ± 0.05	<b>0.002</b>	778 ± 57	803 ± 83	0.27
SLF anterior	0.43 ± 0.05	0.39 ± 0.04	<b>0.01</b>	772 ± 74	780 ± 81	0.75
SLF posterior	0.54 ± 0.06	0.51 ± 0.08	0.32	737 ± 46	753 ± 47	0.28
SLF superior	0.62 ± 0.06	0.58 ± 0.06	<b>0.04</b>	690 ± 36	719 ± 49	<b>0.04</b>
AC	0.45 ± 0.04	0.46 ± 0.06	0.54	822 ± 73	810 ± 67	0.60
PC	0.57 ± 0.06	0.55 ± 0.06	0.25	671 ± 49	693 ± 47	0.15
GCC	0.79 ± 0.05	0.77 ± 0.05	0.17	817 ± 40	829 ± 65	0.49
SCC	0.87 ± 0.05	0.86 ± 0.04	0.63	701 ± 86	729 ± 62	0.25
BCC	0.72 ± 0.07	0.63 ± 0.09	<b>0.002</b>	783 ± 87	896 ± 107	<b>0.001</b>

CST = corticospinal tracts at the level of the pons; MCP = middle cerebellar peduncle; SCP = superior cerebellar peduncle; GIC = genu of the internal capsule; PIC = posterior limb of the internal capsule; UNC = uncinate fasciculus; ILF = inferior longitudinal fasciculus; SLF = superior longitudinal fasciculus; AC = anterior cingulum; PC = posterior cingulum; GCC = genu of corpus callosum; SCC = splenium of corpus callosum; BCC = body of corpus callosum.